Estimation of elastic parameters, mineralogy and pore characteristics of Gondwana shale in Eastern India for evaluation of shale gas potential

Piyush Sarkar[1,*], Kumar Hemant Singh[1], Ranjana Ghosh[2] and Trilok Nath Singh[1]

[1]Department of Earth Sciences, Indian Institute of Technology Bombay, Mumbai 400 076, India
[2]National Geophysical Research Institute, Hyderabad 500 007, India

Studies on resource potential of unconventional reservoirs are drawing the attention of scientific community since the last couple of decades. Because of low permeability of shale, the production demands hydraulic fracturing in shale layers. Brittleness index gives an idea on the toughness of shale layers and helps in setting the parameters for hydraulic fracturing. Elastic properties such as Young's modulus are important parameters for building geo-mechanical models for rock strata which are essential for several applications related to mechanical rock failure during well drilling, completion and stimulation. The physical and geochemical properties of Gondwana shale samples from Eastern India were analysed for mineralogy, pore types and dynamic elastic properties using powder X-ray diffraction (XRD), scan electron microscopy (SEM) and ultrasonic velocity measurements respectively. The measured *P*- and *S*-wave velocities and the estimated elastic parameters of Gondwana shale samples show an increase in magnitude with depth indicating the effect of hardness and compaction. The effect of hardness on velocity and elastic parameter is also supported by the increase in quartz percentage in shale with depth. An empirical relationship between *P*- and *S*-wave velocity is proposed for Gondwana shale. The XRD experiments reveal the dominance of clay minerals over non-clay minerals in the samples lower the shear strength of South-Karanpura field, at shallow depth, supported by measured elastic properties. The presence of flaky clay texture/topography and abundant micro (>0.75 μm) and nano (<0.75 μm) pores of various shapes in the samples with organic matter in the SEM images suggests that formations are of high shale gas prospecting zones.

Keywords: Gondwana shale, SEM, shale gas, ultrasonic, XRD.

*For correspondence. (e-mail: piyush.gph@gmail.com)

THERE has been systematic effort in the last few decades to characterize unconventional reservoirs such as shale rock due to ever-increasing demand for energy across the globe. Significant development in unconventional resource has been achieved in countries like US; however in India, where consumption of fuel is increasing steadily, intensive study on this topic has started only recently. At the moment, there is a lot of emphasis on estimating the shale gas potential of the Indian subcontinent[1]. Therefore, the estimation of shale gas potential of a sedimentary basin requires the measurements and analysis of a set of physical properties of shale rock. The significant properties are mineralogy, organic matter abundance, type of maturity, elastic properties, pore types and sizes, porosity and permeability[2]. A systematic analysis of physical properties of rock requires a set of carefully designed laboratory experiments. The laboratory measured petrophysical properties of rock serve as input parameters for predicting variables, constructing a petrophysical model and are used for decision making in many areas of reservoir engineering and petrophysics. To assess the shale gas potential of Gondwana shale and to be able to utilize the properties of shale during production, it is important to characterize the shale samples from ultrasonic *P*- and *S*-wave, powdered XRD and SEM experiments.

The modulus of elasticity (force required to produce unit deformation in a solid), determined from measured ultrasonic velocities, can be crucial while drilling the shale strata. The elastic modulus is also routinely used as input for formation fracturing calculations such as fracture dimension and pressure required to initiate fracturing[2,3].

Shale rock has very low connected porosity and permeability with complex geometry of pores at nanoscale[4,5]. The abundance of pores at nanoscale in shale provides good spaces for fluid accumulation and plays a crucial role in fluid migration[6,7]. Image analysis using SEM is one of the most widely applied approaches for studying the pore structure and surface topography or

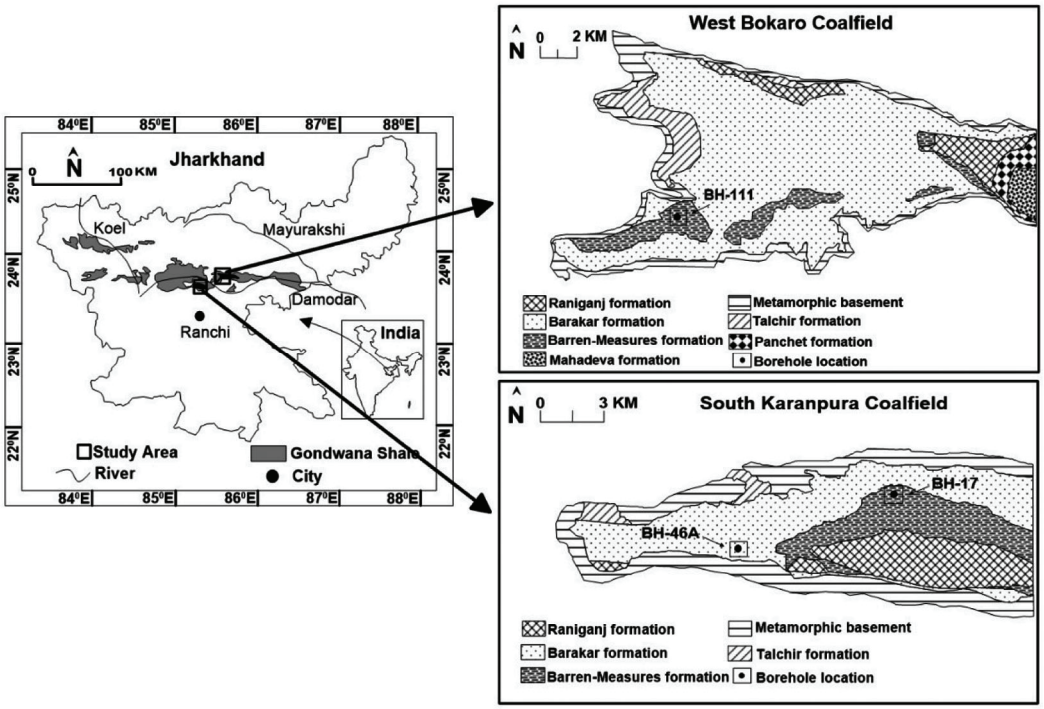

Figure 1. The location of study areas – the South Karanpura and West Bokaro coalfields (after refs 11, 14).

surface texture in a rock sample[8]. The resolution of SEM varies from nanometres to micrometres and the micrographs show the mineral composition, surface topography and pore structure of rock which could be of great significance for evaluation of shale gas potential.

The evaluation of the potential of any reservoir demands a precise mineral analysis. XRD is one of the widely used techniques for qualitative and quantitate mineralogy analysis of fine-grained clay-rich rock like shale[9].

This study shows powder-XRD, SEM and ultrasonic velocity measurements to characterize the shale to understand its physical behaviour. The outcome from each experiment is analysed in the light of primary evaluation of the shale gas potential of the Barakar and Barren Measures Formation in the South-Karanpura and West-Bokaro basin. This will lead to evaluation of seismic wave velocities, elastic moduli, detailed mineralogy, surface topography/texture and pore sizes and shapes dominant in samples. The measured physical properties of this study are important in the context of decision-making during the evaluation and production phase. The results are compared with other important shale gas and oil producing sites in the world.

Study area

The South-Karanpura and West-Bokaro coalfields, located in the Ramgarh district of the Jharkhand state of India (Figure 1), are situated within the Damodar valley and occupy an area of 195 and 215 sq. km respectively[10]. The shale rocks found in both the coalfields belong to lower Gondwana Supergroup. The core samples of shales are collected from various depths of three different bore holes of Urimari block and Pundi block of South Karanpura and West Bokaro coalfield respectively. Eleven samples belong to Barren Measures Formation (Middle Permian) while another five samples represent Barakar Formation (lower Permian).

Gondwana shale belongs to non-marine sedimentary origin. The Barren Measures shale of South-Karanpura coalfield is known for its high shale gas prospective horizon due to the presence of type III kerogen[11], high amount of total organic carbon (TOC) (3.05–9.38%), thickness (~1000 m) and high thermal maturity (>1%)[12]. The Barakar Formation shale has higher TOC (6.89–12.34%) and thermal maturity than Barren Measures shale[13]. The TOC for Barren Measures shale of west-Bokaro coalfield ranges from 2.66% to 6.18% and is dominated by types II and III Kerogen with a thickness of ~750 m (ref. 14). Thermal maturity, high organic matter, thickness and expanse makes Gondwana shales one of the propitious shale gas prospective zones in India.

Laboratory measurements

The laboratory experiments used in this study to characterize the shale samples were ultrasonic velocity, powder

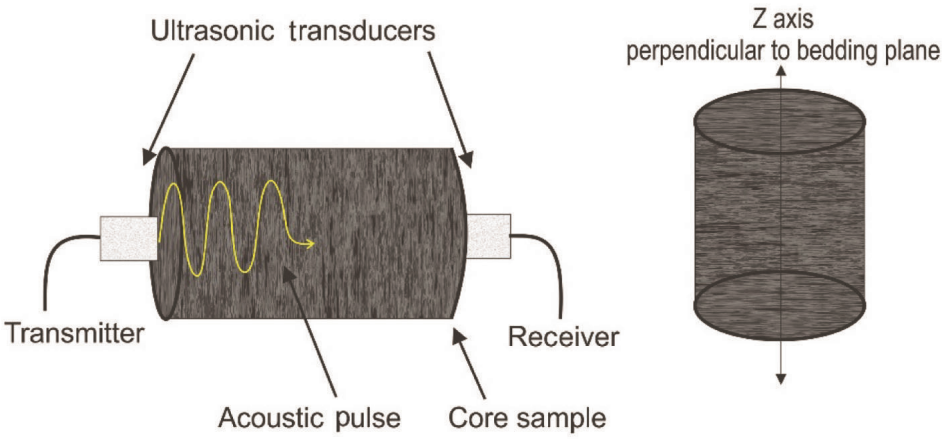

Figure 2. Ultrasonic measurements of core sample normal to the bedding plane.

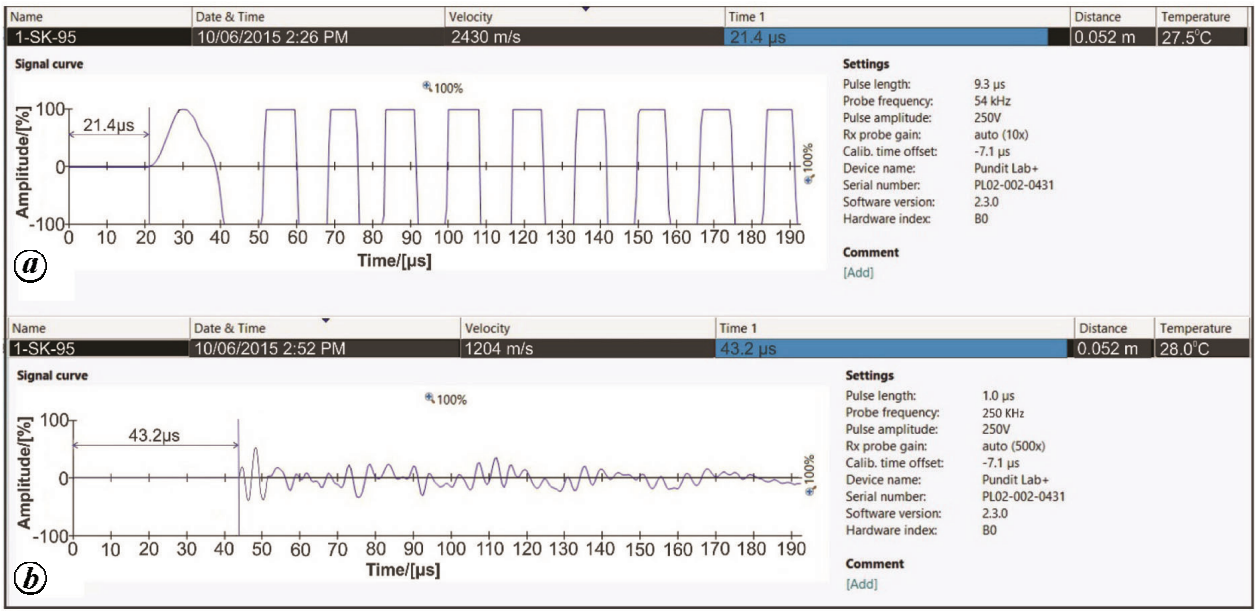

Figure 3. Amplitude % against the time during a typical ultrasonic measurement of (***a***) *P*-wave and (***b***) *S*-wave of the same core sample.

XRD and SEM. These methods are discussed in the following subsections.

Ultrasonic velocity measurement

The ultrasonic velocity testing is a non-destructive way to characterize geological core sample properties at room temperature and pressure. This technique involves measuring the velocity of ultrasonic compressional and shear waves that propagate along the longitudinal axis of the rock sample[15]. The transducers of frequency 54 kHz and 250 kHz were used to generate *P*- and *S*-wave respectively. The physical dimension of the core samples was measured with an accurate digital vernier calliper. The bulk density of the sample was estimated using the measured physical dimensions and weight of the samples. The velocities were measured along the vertical direction (*Z*-axis) of the core samples using Pundit Lab+ instrument (Figure 2). Figure 3 *a* and *b* showed arrival time of *P*- and *S*-waves during the ultrasonic measurements of a core sample. The velocities and density values were then employed to derive the elastic moduli from the following standard equations[16]

$$E = \frac{\rho V_S^2 (3V_P^2 - 4V_S^2)}{(V_P^2 - V_S^2)}, \quad (1)$$

$$K = \frac{\rho(3V_P^2 - 4V_S^2)}{3}, \quad (2)$$

Table 1. Ultrasonic *P*- and *S*-wave velocities and dynamic elastic moduli measured from core samples of Gondwana shale

Depth (m)	V_P (m/s)	V_S (m/s)	V_P/V_S	Shear modulus (μ) (GPa)	Bulk modulus (k) (GPa)	Young's modulus (E) (GPa)
South Karanpura–Barren–Measures Formation						
21	1463	715	2.04	1.23	3.51	3.31
23	1496	731	2.04	1.29	3.68	3.46
47	1610	783	2.05	1.48	4.28	3.98
53	1770	841	2.10	1.71	5.28	4.62
59	1890	887	2.13	1.90	6.08	5.16
South Karanpura–Barakar Formation						
53	2110	1062	1.98	2.67	7.00	7.12
95	2430	1204	2.01	3.44	9.43	9.20
137	3293	1584	2.07	5.95	17.82	16.08
156	3616	1845	1.95	8.08	20.27	21.40
325	3947	2055	1.92	10.02	23.62	26.35
West Bokaro–Barren Measures Formation						
26	1681	824	2.04	1.63	4.61	4.38
35	1696	833	2.03	1.66	4.69	4.47
53	2032	988	2.05	2.34	6.80	6.31
62	2138	1075	1.98	2.77	7.28	7.39
65	2143	1101	1.94	2.91	7.15	7.70
68	2174	1114	1.95	2.98	7.38	7.89

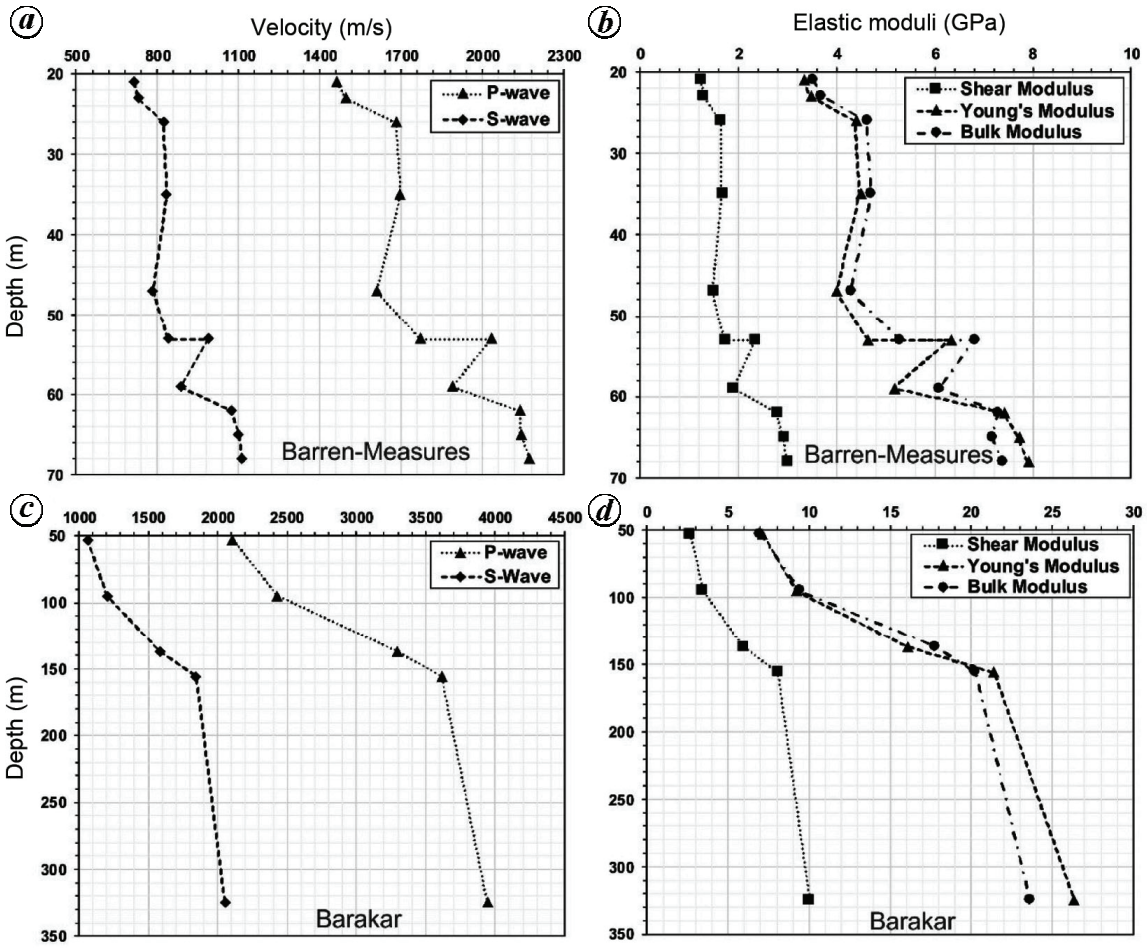

Figure 4. Variation of *P*- and *S*-wave velocities of Gondwana shale for (***a***) Barren Measures and (***c***) Barakar Formation and elastic moduli for (***b***) Barren Measures and (***d***) Barakar Formation with depth of South Karanpura and West Bokaro coalfields.

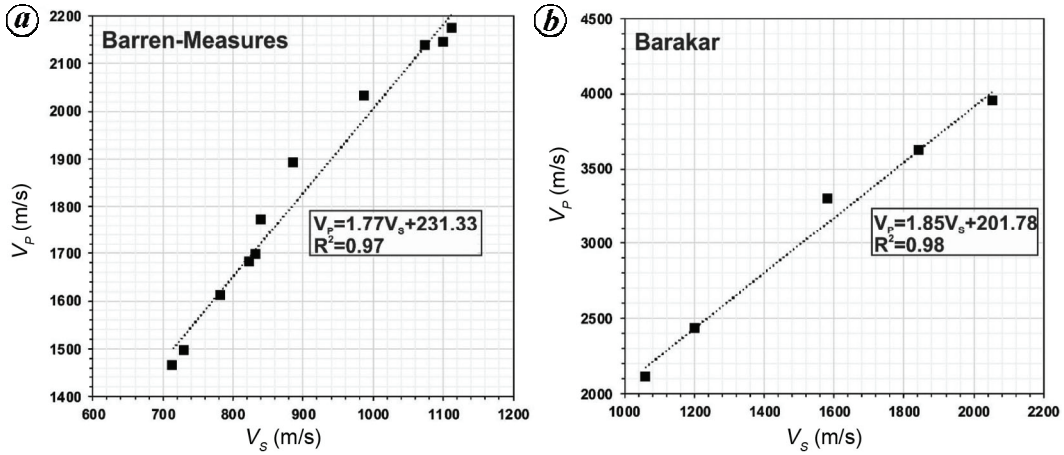

Figure 5. Empirical relationship between *P*- and *S*-wave for Gondwana shale rock of (***a***) Barren Measures and (***b***) Barakar Formation.

$$\mu = \rho V_S^2, \tag{3}$$

where E is the Young's modulus, K the bulk modulus and μ the shear modulus, V_P and V_S are *P*- and *S*-wave velocities and ρ the density.

Powder X-ray diffraction

The X-ray diffractometer ('Empyrean', Malvern *P* analytical), based on the idea of constructive interference of monochromatic X-ray and crystalline material, can identify different mineral phases in the powdered shale samples where each mineral has its own unique fingerprint[17,18]. In our experiment, the powder sample was prepared by grinding the rock sample to a fine powder of size less than 10 μm (or 200-mesh) with agate mortar and pestle.

The X-ray diffracts with different intensity for different lattice plane spacing d and angle of incidence theta (θ) for different minerals. The peak of X-ray intensity corresponding to θ and 2θ was then analysed. The θ and 2θ are the angles moved by the sample and the detector with respect to Bragg's plane respectively. Bragg's equation was then used to estimate the *d*-spacing value corresponding to every peak position for the known wavelength λ of the beam[19]. The unknown mineral was then identified by matching their *d*-spacing values with the *d*-spacing values of known mineral databases. The software HIGH SCORE PLUS 4.0 was used for processing of XRD data.

Scan electron microscopy

The SEM (JSM '6390' JEOL and 'Ultra 55' CARL ZESSIS) was used to generate a high resolution 2D raster micrograph, by bombarding the electron beams on the surface of a rock sample and detecting the scattered electron beams[20,21]. These high resolution SEM micrographs reveal features like mineral grains, pore types and size, on a scale of micrometre to nanometre present in the sample.

Results and discussion

On the basis of the above mentioned laboratory experiments, the measured and estimated parameters and features of Gondwana shale are presented and discussed. They are compared with the shale parameters and features from other parts of the world which already produce shale gas and oil.

Velocity and dynamic elastic moduli

The measured compressional (V_P) and shear wave (V_S) velocities from ultrasonic experiments are shown in Table 1. Figure 4 *a* and *c* shows that the velocity of Gondwana shale increases with depth for both the formations. The average density of shale samples was estimated in the laboratory for both the formations. The average bulk density value of shale for Barakar Formation of South Karanpura coalfield is 2.375 g/cc while for Barren Measures of South Karanpura and West Bokaro coalfields are 2.413 g/cc and 2.405 g/cc respectively. The elastic moduli calculated from these ultrasonic velocities and density using eqs (1)–(3) are presented in Table 1. Figure 4 *b* and *d* shows that the elastic moduli of shale for both the formations increase with depth. The curves also indicate that the estimated elastic moduli follow the trend exhibited by the ultrasonic velocity curves (Figure 4 *a* and *c*). An empirical relationship between *P*- and *S*-wave velocity for Gondwana shale of Barren measures and Barakar Formation is proposed with R^2 (goodness of fit) value 0.97 (eq. (4)) and 0.98 (eq. (5)) respectively. These

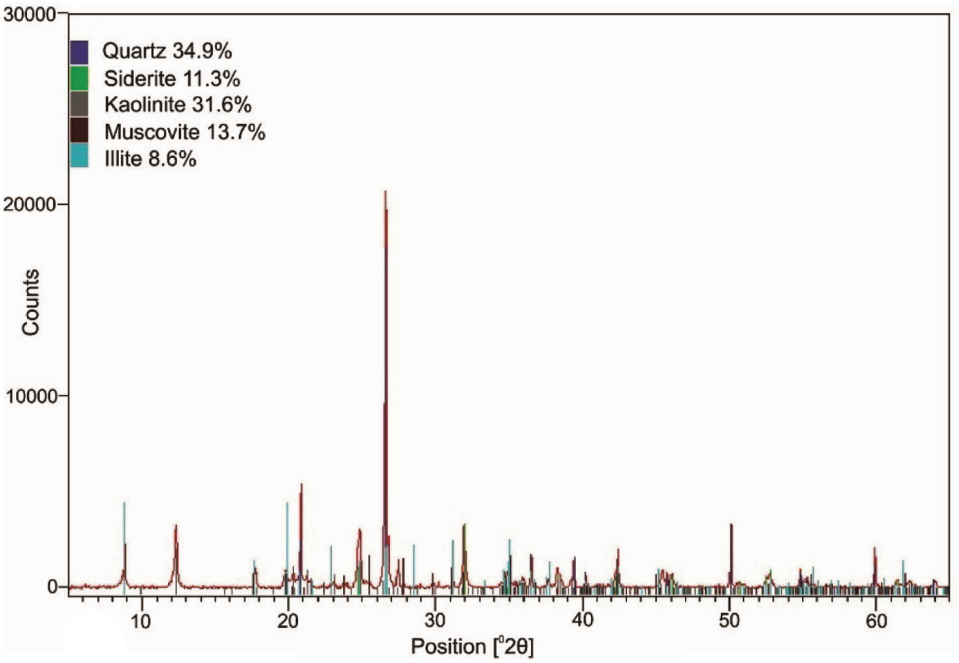

Figure 6. The XRD peaks for shale rock sample (156 m depth) of Barakar Formation.

Table 2. Estimated *t*-stat and *P*-value of linear relationship between V_P and V_S for shale

Formation	*t*-stat	*P*-value
Barren–Measure shale	14.78	1.28E-07
Barakar shale	15.11	6.28E-04

linear empirical relations are proposed by analysing the regression line between V_P and V_S (Figure 5). The *t*-stat and *P* value of the linear relationship between V_P and V_S for Barakar and Barren Measures shale are shown in Table 2. Statistical significance of correlation between *P*- and *S*-wave velocity was tested by assuming a null hypothesis that there is no significant linear relationship (correlation) between V_P and V_S in the population. Since for Barren Measures shale, the *P*-value = 1.28E-07 < 0.001 = α, and for Barakar shale, *P*-value = 0.00062 < 0.001 = α level of significance, the null hypothesis is rejected and it is found that there is a statistically significant linear relationship between V_P and V_S of Barakar and Barren Measures shale.

$$V_P = 1.77 \times V_S + 231.33, \quad (4)$$

$$V_P = 1.85 \times V_S + 201.78. \quad (5)$$

The measured velocities for both Barakar and Barren Measures shale are similar to those estimated for Mesaverde shale[22], Dog Creek shale[23], Wills Point shale[23], Pierre shale[24], Marcellus shale[25] and Eagle Ford shale[26]. This comparison is shown in Table 3.

Shale mineralogy and brittleness index

Figure 6 represents the X-ray diffraction intensity pattern for different peak positions for different minerals present in one of the Gondwana shale samples. The mineralogy obtained from XRD experiments may be classified as clay minerals and non-clay minerals according to their unique 2θ and *d* spacing values. The identified clay minerals are Kaolinite and Illite while the non-clay minerals are quartz, siderite, muscovite and orthoclase. The standard 2θ values for primary shale minerals[27] are listed in Table 4.

The clay mineral (kaolinite + illite) in the shale samples from Barakar Formation varies from 38.3% to 58.7% by volume whereas the non-clay minerals (quartz + siderite + muscovite + orthoclase) vary from 41.3% to 61.7% by volume. The volume percentage of clay and non-clay minerals for Barren Measures Formation varies from 21.3% to 53.7% and 46.3% to 78.7% respectively (Table 5).

The percentage of quartz in the shale samples increases with depth (Table 5). As the hardness of quartz is 7 on mohoscale, it elevates the hardness of the shale sample with depth. Evaluation of petrophysical properties of shale is very tedious due to variation in its mineralogy. Figure 7 is a ternary plot representing the variation in the total fraction of quartz, clay and carbonate in the Gondwana Shale of Barakar and Barren Measures Formation. The presence of a large amount of clay in shale affects the pore structure and may enhance the adsorption ability of shale rock for methane as well[11]. The presence of non-clay minerals such as quartz, mica and carbonate is key to estimating the brittleness index (BI) of the shale rock.

Table 3. A comparison of *P*- and *S*-wave velocities of Gondwana shale with those obtained for shales from different parts of the globe

Shale type	V_P (m/s)	V_S (m/s)	Depth (m)
Mesaverde shale[22]	3749	2621	1184
Dog creek shale[23]	1875	826	143.3
Wills point shale[23]	1058	387	58.3
Pierre shale[24]	2074	869	450
Marcellus shale[25]	2865–3658	1825–2244	1850–1890
Eagle ford shale[26]	3110	2010	Outcrop sample
Gondwana shale	2110–3947 (Barakar)	1062–2055 (Barakar)	53–325
	1463–2174 (Barren Measures)	715–1114 (Barren Measures)	21–68

Table 4. Shale minerals with standard 2θ values used for XRD analysis[27]

Minerals	2θ (deg)
Quartz	20.9, 26.6
Kaolinite	12.3, 24.8
Illite	8.8, 19.8
Siderite	31.9
Muscovite	8.8
Orthoclase	27.4

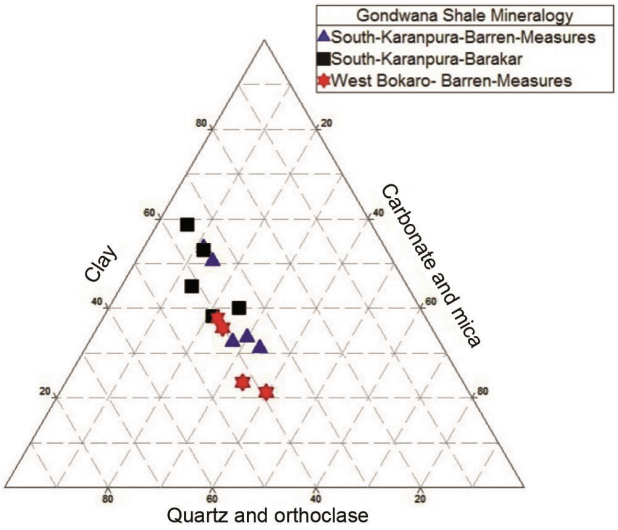

Figure 7. Ternary diagram for mineralogy of Gondwana shale.

BI is a measure of the rock's ability to fracture and depends on diagenesis, mineral composition, TOC, lithology, thermal maturity effective stress, porosity, type of fluid, etc.[28–30].

The BI of shale is defined in several studies based on the mineralogical composition[30,31]. In this article, little modification is proposed over Jarvie's formula[31] for brittleness index (BI) of Gondwana shale by including the effect of mica and carbonate (eq. (6)). Therefore, the modified BI of the Gondwana shale strata, based on its mineralogy composition, is proposed as

$$\mathrm{BI_{Shale}} = \frac{(\text{quartz} + \text{mica} + \text{carbonate})}{(\text{quartz} + \text{clay} + \text{carbonate} + \text{mica})} \times 100. \qquad (6)$$

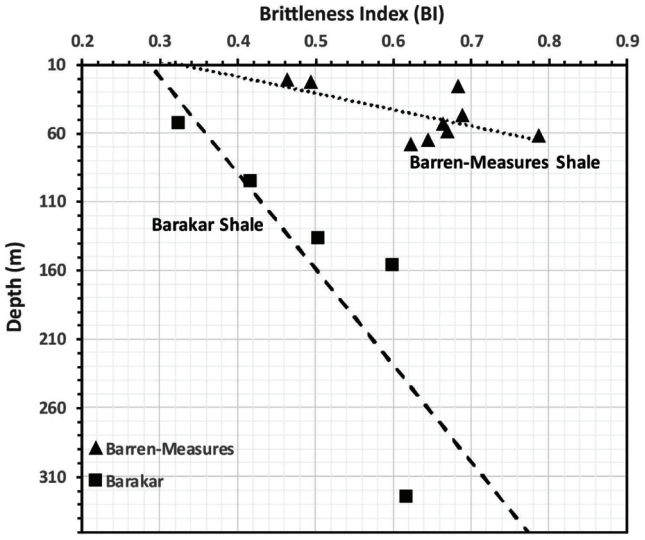

Figure 8. Brittleness index (BI) of Gondwana shale of Barren Measures and Barakar Formation.

The BI of Barren Measures shale varies from 0.46 to 0.78 for South Karanpura and West Bokaro sub-basin. For Barakar Formation of South Karanpura basin, the BI varies from 0.32 to 0.61 (Figure 8).

The average BI for Barren Measure shale is 0.63 up to the depth of 70 m whereas the average BI for Barakar shale is 0.49 up to the depth of 325 m. The measured BI values for Barakar and Barren-Measures shale are at the higher end of the brittleness range classified by Altamar *et al.*[32] for Barnett shale.

The identified mineralogy of Gondwana shale for Barren Measures and Barakar Formation shows that the volume percentage of quartz and clay minerals in the samples is similar to those of Bazhenov shale[33], Murteree shale[34], Eagleford shale[35], Marcellus shale[36–39] and Middlesex shale[36] (Table 6).

Pore characterization

In any unconventional reservoir like shale, the study on pore size and the connectivity between the pore bodies is important for understanding the storing

Table 5. Average mineralogy of Gondwana shale in the samples

Average mineralogy (volume %)						
Depth (m)	Clay	Quartz	Muscovite	Orthoclase	Siderite	Rutile
South Karanpura–Barren Measures Formation						
21	53.7	34.9	9.8	–	1.6	–
23	50.7	34.6	10.9	–	3.8	–
47	31.1	35.4	16.6	–	16.9	–
53	33.5	36.6	26.4	–	3.4	–
59	32.2	39.6	23.6	–	3.7	0.9
South–Karanpura–Barakar Formation						
53	58.7	22.4	2.5	13.0	3.3	–
95	53.1	26.2	11.8	9.0	–	–
137	44.9	32.2	13.3	9.4	0.2	–
156	40.2	34.9	13.7	–	11.3	–
325	38.3	40.8	18.9	–	2.0	–
West Bokaro–Barren Measures Formation						
26	23.4	34.2	12.9	8.3	21.2	–
62	21.3	39.0	23.1	–	16.6	–
65	35.6	40.2	18.4	–	5.8	–
68	37.8	40.2	19.1	–	2.9	–

Table 6. A comparison of average mineralogy of Gondwana shales with those obtained for shales from different parts of the globe

Shale type	Quartz (volume %)	Clay (volume %)
Bazhenov shale[33]	46.0	48.0
Murteree shale[34]	42.78	43.05
Eagle ford shale[35]	20.0	20.0
Marcellus shale[36–39]	20.0–77.0	5.0–60.0
Middlesex shale[36]	25.0	65.0
Gondwana shale	22.4–40.8 (Barakar) 34.2–40.2 (Barren Measures)	38.3–58.7 (Barakar) 21.3–53.7 (Barren Measures)

Table 7. A comparison of pore sizes and shapes distribution of Gondwana shale with those obtained for shales from different parts of the globe

Shale type	Size of nano pores (nm)	Shapes
Barnett shale[4,40,41]	5–750	Irregular, bubble-like, elliptical
Continental shale-North China[42–44]	2–35	Irregular, elliptical
Woodford shale[45]	2–300	Irregular, elliptical elongated
Haynesville shale[45]	2–300	Irregular, elliptical, circular
Gondwana shale	2–500	Circular, oval, irregular, elongated

and flow mechanism of oil and gas. SEM images show texture, topography, pore types, pore shape and pore size of the shale rock samples (Figure 9). Figure 9 *a* is an field emission scanning electron microscope (FE-SEM) image, which shows the presence of organic matter in the sample. Figure 9 *b* shows the presence of quartz grains along with flaky clay particles in the samples. In this study two types of pore bodies, i.e. intra-particle pores and inter-particle pores are found within the clay mineral grains and between the edges of quartz and clay minerals respectively (Figure 9 *b* and *c*). Both micro (>0.75 μm) and nano (<0.75 μm) pore sizes are analysed in the sample. The organic matter (OM) nanopores of different shapes are identified in the samples. The size of OM nano-pores varies approximately from 2 nm to 500 nm in the sample (Figure 9 *a*). The micro and nanopores are circular, oval, elongated and irregular in shape (Figure 9 *c* and *d*). Few microfractures are also present in the sample (Figure 9 *d*). The OM pore size and pore shapes for Gondwana shale are similar to those experimentally found for Barnett shale in North America[4,40,41], continental shale of

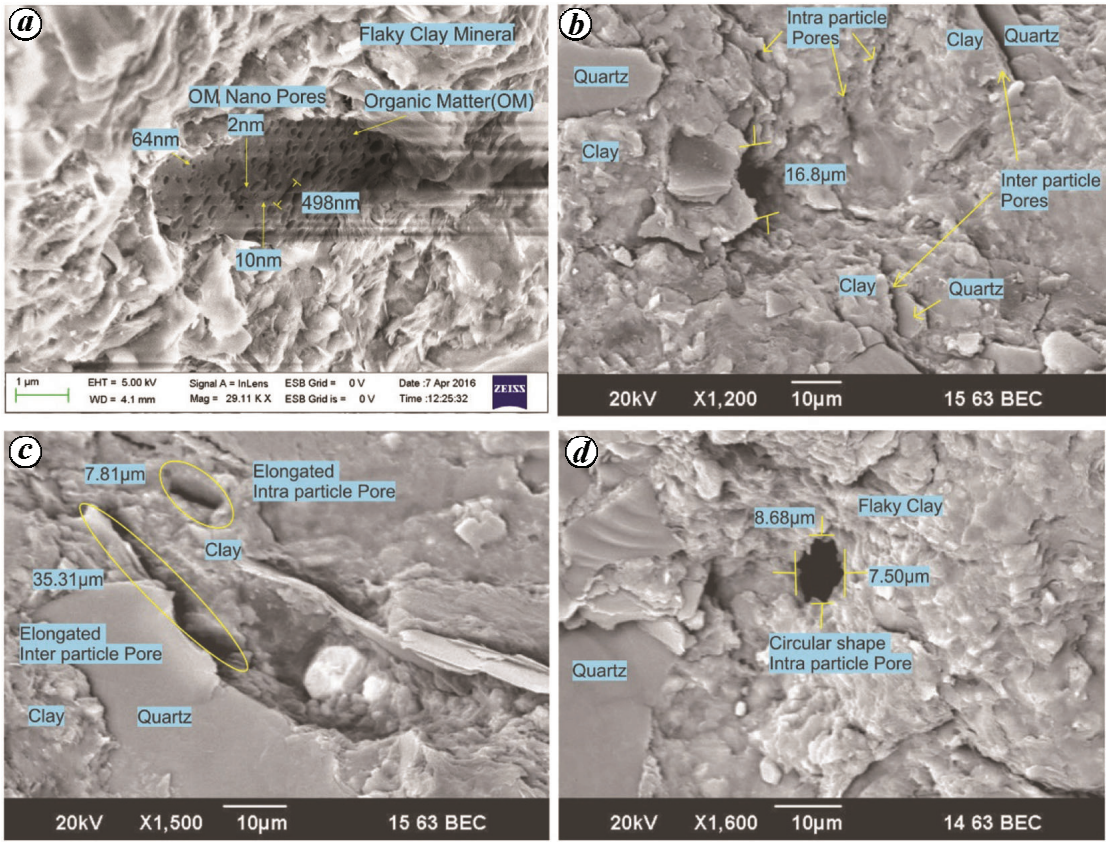

Figure 9. SEM images displaying: (***a***) Presence of organic matter (OM) in shale and the associated oval shape at OM nanopore scale; (***b***) Inter-particle and intra-particle micropores; (***c***) Elongated intra- and inter-particle micropores; (***d***) Circular shape intra-particle micropores.

North China[42–44], Woodford shale[45] and Haynesville shale[45] (Table 7).

Conclusion

Ultrasonic *P*- and *S*-wave velocity measurements, XRD and SEM experiments were conducted to ascertain the physical properties of Gondwana shales. Based on the experimental analysis it was observed that the velocity of Barren Measures shale was lower than the Barakar shale, which helps to draw a conclusion that the Barakar shale is relatively harder, compact and dense. The study of compaction effect is important since shale undergoes transformation in physical structure due to compaction including the diagenetic changes that occur because of chemical and mineralogical changes. Therefore, for thick shale sequences such compaction may cause significant tectonic movement which may produce shale diapirs. The proposed empirical relations between *P*- and *S*-wave velocities are important to understand the elastic behaviour such as Poisson's ratio and fluid factor of shale rock of the region. However, these empirical relations can be used in other areas having similar tectonic evaluation and morphology.

The swelling clays (i.e. bentonite and smectite) are not found in the samples. Absence of swelling clay is favourable as it may react with the fracturing fluid and negatively impact the well performance. The percentage of quartz in shale increases with depth which also supports the increasing effect of compactness and hardness with depth as inferred from velocity and elastic parameters. The fraction of clay minerals in shale samples from the South Karanpura coalfield is high at shallow depths while it is lower for the same depths in West Bokaro coalfield. Since weathering agents transform the wet shale into a clay-rich soil of very low shear strength, the probability of a landslide due to overloading or excavation may trigger failure at sites in South Karanpura coalfield due to high clay content in shale.

Average brittleness of Gondwana shale samples is moderate to high. Barren Measures shale is comparatively more brittle than Barakar shale. The empirical relation of BI is specifically proposed for Gondwana shale of Eastern India, which can be used in other areas of similar geology. The FE-SEM image reveals the presence of organic matter and OM nanopores of varying shapes and sizes (nanometre to micrometre) in the shale samples. The abundance of organic matter pores is important

because they can potentially absorb and store free gas and play a crucial role in migration of gas.

On the basis of measured and observed properties of Gondwana shale of South Karanpura and West Bokaro coalfields and the comparison of their physical properties with oil and gas producing shale in other parts of globe, it is found that the physical behaviour of Gondwana shale is more or less similar. Though the organic richness is high, the maturity, storage capacity etc. needs to be evaluated to ensure that they are potential shale plays.

1. Sain, K., Rai, M. and Sen, M. K., A review on shale gas prospect in Indian sedimentary basins. *J. Indian Geophys. Union*, 2014, **18**, 183–194.
2. Josh, M., Esteban, L., Piane, C. D., Sarout, J., Dewhurst, D. N. and Clennell, M. B., Laboratory characterisation of shale properties. *J. Petrol. Sci. Eng.*, 2012, **88**, 107–124; doi:10.1016/j.petrol.2012.01.023.
3. Hornby, B. E., Experimental laboratory determination of the dynamic elastic properties of wet, drained shales. *J. Geophys. Res.*, 1998, **103**, 29945–29964; doi:10.1029/97jb02380.
4. Loucks, R. G., Reed, R. M., Ruppel, S. C. and Jarvie, D. M., Morphology, genesis, and distribution of nanometer-scale pores in siliceous mudstones of the Mississippian Barnett Shale. *J. Sediment. Res.*, 2009, **79**, 848–861; doi:10.2110/jsr.2009.092.
5. Kuila, U. and Prasad, M., Specific surface area and pore-size distribution in clays and shales. *Geophys. Prospect.*, 2013, **61**, 341–362; doi:10.1111/1365-2478.12028.
6. Ross, D. J. and Bustin, R. M., The importance of shale composition and pore structure upon gas storage potential of shale gas reservoirs. *Mar. Petrol. Geol.*, 2009, **26**, 916–927; doi:10.1016/j.marpetgeo.2008.06.004.
7. Taixian, Z., Characteristics of pore structure of marine shales in South China. *Natural Gas Indus.*, 2012, **32**, 1–4; doi:10.3787/j.issn.1000-0976.2012.09.001.
8. Krinsley, D. H., Pye, K., Boggs Jr, S. and Tovey, N. K., *Backscattered Scanning Electron Microscopy and Image Analysis of Sediments and Sedimentary Rocks*, Cambridge University Press, 2005.
9. Moecher, D. P., Characterization and identification of mineral unknowns: a mineralogy term project. *J. Geosci. Educ.*, 2004, **52**, 5–9; doi:10.5408/1089-9995-52.1.5.
10. Konar, B. B., Banerjee, S. B., Chaudhuri, S. G., Choudhury, A., Das, N. S. and Sen, K., In *Coal Preparation*, Allied Publishers Ltd, New Delhi, India, 1997.
11. Mendhe, V. A., Kamble, A. D., Bannerjee, M., Mishra, S., Mukherjee, S. and Mishra, P., Evaluation of shale gas reservoir in Barakar and Barren Measures formations of north and south Karanpura Coalfields, Jharkhand. *J. Geol. Soc. India*, 2016, **88**, 305–316; doi:10.1007/s12594-016-0493-7.
12. Tewari, A. and Dutta, S., Organic geochemistry and pore system characterization of gas shales: an example from the lower Gondwana shales, eastern India. In Proceedings of Society for Organic Petrology, Sydney, Australia, 2014, vol. 31, p. 154.
13. Mukhopadhyay, G., Mukhopadhyay, S. K., Roychowdhury, M. and Parui, P. K., Stratigraphic correlation between different Gondwana basins of India. *J. Geol. Soc. India*, 2010, **76**, 251–266; doi:10.1007/s12594-010-0097-6.
14. Tewari, A., Dutta, S. and Sarkar, T., Organic geochemical characterization and shale gas potential of the Permian Barren measures formation, West Bokaro sub-basin, eastern India. *J. Petroleum Geol.*, 2016, **39**, 49–60; doi:10.1111/jpg.12627.
15. McSkimin, H. J., Ultrasonic methods for measuring the mechanical properties of liquids and solids. In *Physical Acoustics* (ed. Mason, W. P.), Academic Press, 1964, vol. 1, pp. 271–334; doi:10.1016/B9781-1-4832-2857-0.50010-1.
16. Yilmaz, O. Z., Engineering Seismology with Applications to Geotechnical Engineering. Society of Exploration Geophysicist, Tulsa, OK, USA, 2015; doi:10.1190/1.9781560803300.
17. Moore, D. M. and Reynolds, R. C., *X-ray Diffraction and the Identification and Analysis of Clay Minerals*, Oxford University Press, New York, 1997.
18. Srodon, J., Drits, V. A., McCarty, D. K., Hsieh, J. C. and Eberl, D. D., Quantitative X-ray diffraction analysis of clay-bearing rocks from random preparations. *Clays Clay Miner.*, 2001, **49**, 514–528; doi:10.1346/ccmn.2001.0490604.
19. Bragg, W. L., The structure of some crystals as indicated by their diffraction of X-rays. *Proc. R. Soc. Lond A: Math., Phys. Eng. Sci.*, 1913, **610**, 248–277; doi:10.1098/rspa.1913.0083.
20. Reimer, L., Scanning electron microscopy: physics of image formation and microanalysis, Springer-Verlag, Berlin, Heidelberg, 2000; doi:10.1088/0957-0233/11/12/703.
21. Goldstein, J. *et al.*, *Scanning Electron Microscopy and X-ray Microanalysis: A Text for Biologists, Materials Scientists, and Geologists*, Springer Science and Business Media, New York, 2003; doi:10.1007/978-1-4613-0491-3.
22. Lin, W., Ultrasonic velocities and dynamic elastic moduli of Mesaverde rocks. Lawrence Livermore Nat. Lab. 20273, CA, USA, 1985; https://www.osti.gov/scitech/biblio/5915663-ultrasonic-velocitiesdynamic-elastic-moduli-mesaverde-rocks-revision
23. Robertson, J. D. and Corrigan, D., Radiation patterns of a shear-wave vibrator in near-surface shale. *Geophysics*, 1983, **48**, 19–26. doi:10.1190/1.1441401.
24. White, J. E., Martineau-Nicoletis, L. and Monash, C., Measured anisotropy in Pierre shale. *Geophys. Prospect.*, 1983, **31**, 709–725; doi:10.1111/j.1365-2478.1983.tb01081.x.
25. Roy, S., Near-surface characterization via seismic surface-wave inversion, Ph D diss., Department of Earth and Atmospheric Sciences, University of Houston, Houston, 2013.
26. Stewart, R. R., Ruiz, F., Wellner, J., Dyaur, N. and Huang, L., Exploration geophysics at the University of Houston: the shale trail and other unconventional voyages. *Recorder.*, 2015, **40**, 32–37; https://csegrecorder.com/assets/pdfs/2015/2015-09-RECORDER_University_of_Houston.pdf
27. Breeden, D. and Shipman, J., Shale analysis for mud engineers. AADE-04-DF-HO-30. Drilling fluids conference, Astrodome, Houston, Texas, 2004, pp. 1–17.
28. Handin, J., Hager, R. V., Friedman, M. and Feather, J. N., Experimental deformation of sedimentary rocks under confining pressure: Pore pressure tests. *AAPG Bull.*, 1963, **47**, 717–755.
29. Davis, D. and Reynolds, S. J., *Structural Geology of Rocks and Regions*, Wiley and Sons, New York, 1996.
30. Wang, F. P. and Julia, F. W., Screening criteria for shale-gas systems. *Gulf Coast Assoc. Geol. Soc. Trans.*, 2009, **59**, 779–793.
31. Jarvie, D. M., Hill, R. J., Ruble, T. E. and Pollastro, R. M., Unconventional shale-gas systems: the Mississippian Barnett Shale of north-central Texas as one model for thermogenic shale-gas assessment. *Am. Assoc. Pet. Geol. Bull.*, 2007, **91**, 475–499; doi:10.1306/12190606068.
32. Perez Altamar, R. and Marfurt, K., Mineralogy-based brittleness prediction from surface seismic data: application to the Barnett Shale. *Interpretation*, 2014, **2**, T255–T271; doi:10.1190/INT-2013-0161.1.
33. Vernik, L. and Landis, C., Elastic anisotropy of source rocks: implication for hydrocarbon generation and primary migration. *Am. Assoc. Pet. Geol. Bull.*, 1996, **80**, 531–544; doi:10.1306/64ed8836-1724-11d7-8645000102c1865d.
34. Ahmad, M. and Haghighi, M., Mineralogy and petrophysical evaluation of Roseneath and Murteree shale formations, Cooper basin, Australia using QEMSCAN and CT scanning. In *SPE Asia*

Pacific Oil and Gas Conference and Exhibition, Society of Petroleum Engineers, 2012; doi:10.2118/158461-MS.
35. Martin, R., Baihly, J. D., Malpani, R., Lindsay, G. J. and Atwood, W. K., Understanding production from Eagle Ford-Austin chalk system. In *SPE Annual Technical Conference and Exhibition*, Society of Petroleum Engineers, 2011; doi:10.2118/145117-MS.
36. Hosterman, J. W. and Whitlow, S. I., Clay mineralogy of Devonian shales in the Appalachian Basin (#1298). USGS Publications Warehouse, 1983; http://pubs.usgs.gov/pp/1298/report.pdf
37. Enomoto, C. B., Coleman Jr, J. L., Swezey, C. S., Niemeyer, P. W. and Dulong, F. T., Geochemical and mineralogical sampling of the Devonian shales in the Broadtop Synclinorium, Appalachian Basin, in Virginia, West Virginia, Maryland, and Pennsylvania (#2015-1061). USGS Publications Warehouse, 2015; https://pubs.er.usgs.gov/publication/ofr20151061
38. Vernik, L., Seismic petrophysics in quantitative interpretation. Society of Exploration Geophysicists, Tulsa, OK, USA, 2016; doi:10.1190/1.9781560803256.
39. Wang, G. and Carr, T. R., Organic-rich Marcellus Shale lithofacies modeling and distribution pattern analysis in the Appalachian Basin. *Am. Assoc. Pet. Geol. Bull.*, 2013, **97**, 2173–2205.
40. Loucks, R. G., Reed, R. M., Ruppel, S. C. and Hammes, U., Spectrum of pore types and networks in mudrocks and a descriptive classification for matrix-related mudrock pores. *Am. Assoc. Pet. Geol. Bull.*, 2012, **96**, 1071–1098; doi:10.1306/08171111061.
41. Slatt, R. M. and O'Brien, N. R., Pore types in the Barnett and Woodford gas shales: contribution to understanding gas storage and migration pathways in fine-grained rocks. *Am. Assoc. Pet. Geol. Bull.*, 2011, **95**, 2017–2030; doi:10.1306/03301110145.
42. Er, C., Zhao, J. Z., Bai, Y. B., Fan, H. and Shen, W. X., Reservoir characteristics of the organic-rich shales of the Triassic Yanchang Formation in Ordos Basin. *Oil Gas Geol.*, 2013, **34**, 708–716; doi:10.11743/ogg20130519.
43. Xiangzeng, W., Shengli, G. and Chao, G., Geological features of Mesozoic lacustrine shale gas in south of Ordos Basin, NW China. *Petrol. Exp. Develop.*, 2014, **41**, 326–337; doi:10.1016/S1876-3804(14)60037-9.
44. Zeng, W. T., Zhang, J. C., Ding, W. L., Wang, X. Z., Jiu, K. and Fu, J. L., Characteristics and influence factors of nanopores in Yanchang Shale reservoir: a case study of Liuping-171 well in Erdos Basin. *J. China Coal Soc.*, 2014, **39**, 1118–1126; doi:10.13225/j.cnki.jccs.2013.0842.
45. Chalmers, G. R., Bustin, R. M. and Power, I. M., Characterization of gas shale pore systems by porosimetry, pycnometry, surface area, and field emission scanning electron microscopy/transmission electron microscopy image analyses: examples from the Barnett, Woodford, Haynesville, Marcellus, and Doig units. *Am. Assoc. Pet. Geol. Bull.*, 2012, **96**, 1099–1119; doi:10.1306/10171111052.

ACKNOWLEDGEMENTS. We thank IIT Bombay, India for providing adequate laboratory facilities for the research work. We also thank Coal India Ltd and Prof. S. Dutta for kindly providing the shale samples. We also thank MHRD, Government of India for providing financial support.

Received 23 August 2017; revised accepted 2 May 2018

doi: 10.18520/cs/v115/i4/710-720